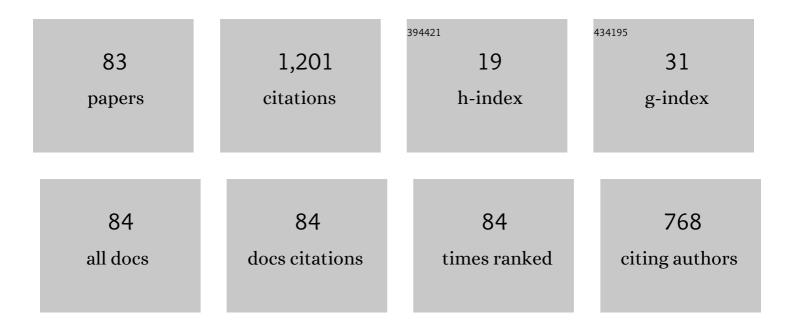
List of Publications by Year in descending order

Source: https://exaly.com/author-pdf/2105493/publications.pdf Version: 2024-02-01



MASANORI HARA

#	Article	IF	CITATIONS
1	Deuterium trapping at defects created with neutron and ion irradiations in tungsten. Nuclear Fusion, 2013, 53, 073006.	3.5	99
2	Trapping of hydrogen isotopes in radiation defects formed in tungsten by neutron and ion irradiations. Journal of Nuclear Materials, 2013, 438, S114-S119.	2.7	76
3	Irradiation effect on deuterium behaviour in low-dose HFIR neutron-irradiated tungsten. Nuclear Fusion, 2015, 55, 013008.	3.5	61
4	The deuterium depth profile in neutron-irradiated tungsten exposed to plasma. Physica Scripta, 2011, T145, 014051.	2.5	50
5	Overview of the US–Japan collaborative investigation on hydrogen isotope retention in neutron-irradiated and ion-damaged tungsten. Fusion Engineering and Design, 2012, 87, 1166-1170.	1.9	43
6	Kinetics and mechanism of hydrogen-induced disproportionation of ZrCo. Fusion Engineering and Design, 2000, 49-50, 831-838.	1.9	42
7	Comparison of deuterium retention for ion-irradiated and neutron-irradiated tungsten. Physica Scripta, 2011, T145, 014050.	2.5	42
8	Hydrogen absorption by Pd-coated ZrNi prepared by using Barrel-Sputtering System. Journal of Nuclear Materials, 2003, 320, 265-271.	2.7	40
9	Hydrogen-induced disproportionation of Zr2M (M=Fe, Co, Ni) and reproportionation. Journal of Alloys and Compounds, 2003, 352, 218-225.	5.5	40
10	Phase transition and electrochemical capacitance of mechanically treated manganese oxides. Journal of Alloys and Compounds, 2006, 414, 137-141.	5.5	34
11	Stability of ZrCo and ZrNi to Heat Cycles in Hydrogen Atmosphere. Fusion Science and Technology, 1995, 28, 1437-1442.	0.6	33
12	Surface coating of small SiO2 particles with TiO2 thin layer by using barrel-sputtering system. Thin Solid Films, 2006, 513, 103-109.	1.8	33
13	Tritium retention in nanostructured tungsten with large effective surface area. Journal of Nuclear Materials, 2013, 438, S1142-S1145.	2.7	29
14	Surface coating with various metals on spherical polymer particles by using barrel sputtering technique. Journal of Alloys and Compounds, 2007, 441, 162-167.	5.5	28
15	Magnetic susceptibility of the Pd–Co–H system. Journal of Alloys and Compounds, 2013, 580, S102-S104.	5.5	26
16	Retention of Hydrogen Isotopes in Neutron Irradiated Tungsten. Materials Transactions, 2013, 54, 437-441.	1.2	25
17	New technique for non-destructive measurements of tritium in future fusion reactors. Nuclear Fusion, 2007, 47, S464-S468.	3.5	21
18	Surface coating of small SiO2 particles with a WO3 thin film by barrel-sputtering method. Journal of Alloys and Compounds, 2007, 441, 157-161.	5.5	19

#	Article	IF	CITATIONS
19	Alloying effects on the hydrogen-storage capability of Pd–TM–H (TM=Cu, Au, Pt, Ir) systems. Journal of Alloys and Compounds, 2014, 614, 238-243.	5.5	19
20	Thermodynamic and Magnetic Properties of Pd <sub>0.93</sub> Ag <sub>0.07</sub> Hydride. Materials Transactions, 2007, 48, 3154-3159.	1.2	18
21	Sensing hydrogen in the gas phase using ferromagnetic Pd–Co films. Journal of Alloys and Compounds, 2015, 645, S213-S216.	5.5	17
22	Hydrogenation effect on magnetic properties of Pd–Co alloys. Journal of Magnetism and Magnetic Materials, 2019, 484, 8-13.	2.3	17
23	Applicability of Pd–Cu alloy to self-developing gas chromatography of hydrogen isotopes. Journal of Nuclear Materials, 2007, 367-370, 1096-1101.	2.7	16
24	Defect annealing and thermal desorption of deuterium in low dose HFIR neutron-irradiated tungsten. Journal of Nuclear Materials, 2015, 463, 1005-1008.	2.7	16
25	Magnetic Properties of Palladium and Palladium–Platinum Alloy of Various Hydrogen Content. Materials Transactions, 2006, 47, 2373-2376.	1.2	15
26	Analysis of a tritium enhanced water spectrum between 7200 and 7245 cmâ^'1 using new variational calculations. Journal of Molecular Spectroscopy, 2013, 289, 35-40.	1.2	15
27	Helium retention behavior in simultaneously He+-H2+ irradiated tungsten. Journal of Nuclear Materials, 2018, 502, 289-294.	2.7	15
28	Alloying effect on heat of hydride and deuteride formation for Pd-based binary alloys. Journal of Alloys and Compounds, 2007, 428, 252-255.	5.5	14
29	Cracking behavior and microstructural, mechanical and thermal characteristics of tungsten–rhenium binary alloys fabricated by laser powder bed fusion. International Journal of Refractory Metals and Hard Materials, 2021, 100, 105651.	3.8	14
30	lsotope effects on hydrogen absorption by Pd–4at.%Pt alloy. Journal of Alloys and Compounds, 2002, 340, 207-213.	5.5	13
31	Sensitivity of a specially designed calorimeter for absolute evaluation of tritium concentration in water. Fusion Engineering and Design, 2010, 85, 2045-2048.	1.9	13
32	Crystal structure change of Li2+xTiO3+y tritium breeder under moist air. Journal of Nuclear Materials, 2010, 404, 217-221.	2.7	12
33	Synergistic effects of high energy helium irradiation and damage introduction at high temperature on hydrogen isotope retention in plasma facing materials. Journal of Nuclear Materials, 2020, 533, 152122.	2.7	12
34	Effects of fabrication conditions on the microstructure, pore characteristics and gas retention of pure tungsten prepared by laser powder bed fusion. International Journal of Refractory Metals and Hard Materials, 2021, 95, 105410.	3.8	12
35	A New Kind of Column Materials for Gas Chromatographic Hydrogen Isotope Separation. Fusion Science and Technology, 2005, 48, 144-147.	1.1	11
36	Near-Infrared Spectroscopy of Tritiated Water. Fusion Science and Technology, 2011, 60, 941-943.	1.1	11

#	Article	IF	CITATIONS
37	<i>In situ</i> measurement of alternating current magnetic susceptibility of Pd–hydrogen system for determination of hydrogen concentration in bulk. Review of Scientific Instruments, 2012, 83, 075102.	1.3	11
38	Tritium distributions on W-coated divertor tiles used in the third JET ITER-like wall campaign. Nuclear Materials and Energy, 2019, 18, 258-261.	1.3	10
39	Retention and desorption behavior of tritium in Si related ceramics. Journal of Nuclear Materials, 2013, 438, 22-25.	2.7	9
40	Design of a tritium gas cell for beta-ray induced X-ray spectrometry using Monte Carlo simulation. Fusion Engineering and Design, 2017, 119, 12-16.	1.9	9
41	Hydrogen-Induced Disproportionation of Zr <sub>2</sub> Co. Materials Transactions, JIM, 2000, 41, 1146-1149.	0.9	8
42	Kinetics of Hydrogen Isotope Absorption for Well-Annealed Palladium-Platinum Alloys. Materials Transactions, 2007, 48, 560-565.	1.2	8
43	Comparison of hydrogen isotope retention and irradiation damage behaviors in tungsten and SS-316 with simultaneous C+–D2+ implantation. Fusion Engineering and Design, 2011, 86, 1776-1779.	1.9	8
44	Monte Carlo simulation of tritium beta-ray induced X-ray spectrum in various gases. Fusion Engineering and Design, 2018, 131, 125-129.	1.9	8
45	Alloying effects on the hydride formation of Zr(Mn1â^'xCox)2. International Journal of Hydrogen Energy, 2011, 36, 12333-12337.	7.1	7
46	Effect of substituting elements on hydrogen uptake for Pd–Rh–H and Pd–Ag–H systems evaluated by magnetic susceptibility measurement. International Journal of Hydrogen Energy, 2013, 38, 7569-7575.	7.1	7
47	Deuterium retention behavior in simultaneously He+–D2+ implanted tungsten. Nuclear Materials and Energy, 2018, 16, 76-81.	1.3	7
48	Determination of retained tritium from ILW dust particles in JET. Nuclear Materials and Energy, 2020, 22, 100673.	1.3	7
49	Helium and hydrogen interaction in tungsten simultaneously irradiated by He+-H2+ at high temperature. International Journal of Hydrogen Energy, 2020, 45, 9959-9968.	7.1	7
50	Water Vapor Permeability of Polypropylene. Fusion Science and Technology, 2011, 60, 1471-1474.	1.1	6
51	Measurement of tritium concentration in water by imaging plate. Fusion Engineering and Design, 2012, 87, 965-968.	1.9	6
52	Galet – Benchmark of a Geant4 based application for the simulation and design of Beta Induced X-ray Spectrometry systems. Fusion Engineering and Design, 2019, 143, 91-98.	1.9	6
53	Tritium distribution analysis of Be limiter tiles from JET-ITER like wall campaigns using imaging plate technique and β-ray induced X-ray spectrometry. Fusion Engineering and Design, 2020, 160, 111959.	1.9	6
54	Tritium analysis of divertor tiles used in JET ITER-like wall campaigns by means of <i>β</i> -ray induced x-ray spectrometry. Physica Scripta, 2017, T170, 014014.	2.5	6

#	Article	IF	CITATIONS
55	Development of a tritium separation process using SDGC. Fusion Engineering and Design, 2006, 81, 821-826.	1.9	5
56	Temperature driven hydrogen-induced disproportionation of Zr2Cu. Journal of Alloys and Compounds, 2009, 487, 489-493.	5.5	5
57	Influence of Internal Structure of Semiconductor Detector on Spectrum of X-Rays Induced by Tritium Beta Rays. Fusion Science and Technology, 2020, 76, 327-332.	1.1	5
58	Thermodynamic and Magnetic Properties of GdPd Hydride. Materials Transactions, 2008, 49, 1428-1433.	1.2	4
59	Hydrogen-induced magnetic and structural transformations of GdCu. Journal of Magnetism and Magnetic Materials, 2009, 321, 423-428.	2.3	4
60	Measurement of Highly Tritiated Water by Imaging Plate. Fusion Science and Technology, 2011, 60, 982-985.	1.1	4
61	Evaluation of terminal composition of palladium–silver hydrides in plateau region by electronic structure calculations. Journal of Alloys and Compounds, 2013, 580, S202-S206.	5.5	4
62	Hydrogen sensing ability of Cu particles coated with ferromagnetic Pd–Co layer. International Journal of Hydrogen Energy, 2017, 42, 16305-16312.	7.1	4
63	Standardization of Tritium Measuring Devices Based on a High-Sensitivity Calorimeter. Fusion Science and Technology, 2008, 54, 182-185.	1.1	3
64	Tritiated water permeation and sorption in polyimide film. Journal of Nuclear Materials, 2012, 429, 325-328.	2.7	3
65	Validation of beta ray scintillation spectra in liquid scintillation counter using Geant4 simulation. , 2014, , .		3
66	Development of Tritium Tracer Doped Liquid Fuel Target for Inertial Confinement Fusion at the Gekko XII-LFEX Facility. Fusion Science and Technology, 2020, 76, 464-470.	1.1	3
67	Monte Carlo simulation of the beta-ray induced X-ray spectra of tritium at various depths in solids. Fusion Engineering and Design, 2021, 172, 112814.	1.9	3
68	Inverse isotope effect of ZrMn (x=1.9 or 2.0)-Q2 (Q=H or D) system. Journal of Physics and Chemistry of Solids, 2013, 74, 1174-1178.	4.0	2
69	Dynamics for HT and HTO Recovery through Water Bubbler and CuO Catalyst. Fusion Science and Technology, 2015, 68, 358-361.	1.1	2
70	Appropriate quenching level in modified integral counting method by liquid scintillation counting. Journal of Radioanalytical and Nuclear Chemistry, 2016, 310, 857-863.	1.5	2
71	Applicability of a 100-mL Polyethylene Vial for Low-Level Tritium Measurement Using a Low-Background Liquid Scintillation Counter. Fusion Science and Technology, 2020, 76, 583-588.	1.1	2
72	Tritium Counting Using a Europium Coordination Complex. Fusion Science and Technology, 2017, 71, 496-500.	1.1	1

#	Article	IF	CITATIONS
73	Modification of LSC spectra of 125I by high atomic number elements. Applied Radiation and Isotopes, 2018, 139, 131-136.	1.5	1
74	Adsorption of hydrogen and deuterium on A-type zeolites at 77†K after various heat treatments. Fusion Engineering and Design, 2020, 158, 111701.	1.9	1
75	Magnetism and Electronic Structure Calculations of Pd-TM Alloys and Hydrogen Systems. , 2013, , 1837-1841.		1
76	Tritium Measurement lâ $\in$ "Tritium in Gas, Liquid, and Solid. , 2017, , 137-164.		1
77	Anomalous Hall effect of PdCo alloy thin films to detect low hydrogen concentration in air. International Journal of Hydrogen Energy, 2022, 47, 7491-7498.	7.1	1
78	Dependence of CuO particle size and diameter of reaction tubing on tritium recovery for tritium safety operation. Fusion Engineering and Design, 2016, 113, 313-317.	1.9	0
79	Tritium-doping enhancement of polystyrene by ultraviolet laser and hydrogen plasma irradiation for laser fusion experiments. Fusion Engineering and Design, 2016, 112, 269-273.	1.9	0
80	Quenching Correction with Two-Dimensional Scintillation Spectrum in Tritium Measurement. Fusion Science and Technology, 2020, 76, 163-169.	1.1	0
81	Working environment of tritium analysis for photoluminescence control. Fusion Engineering and Design, 2021, 170, 112679.	1.9	0
82	Tritium behavior in isotropic graphite at room temperature. Fusion Engineering and Design, 2021, 172, 112801.	1.9	0
83	Suitability of a simple sampler using a brass bar for gaseous tritiated water measurement. Fusion Engineering and Design. 2021, 172, 112743.	1.9	0